



A significant increase in wave height in the North Atlantic Ocean over the 20th century



Xavier Bertin ^{*}, Elizabeth Prouteau, Camille Letetrel

UMR 7266 LIENSs CNRS-Université de La Rochelle, Institut du Littoral et de l'Environnement, 2 rue Olympe de Gouges, 17000 La Rochelle, France

ARTICLE INFO

Article history:

Received 21 November 2012

Accepted 21 March 2013

Available online 28 March 2013

Keywords:

wave climate
numerical model
major increase
climate change
coastal erosion

ABSTRACT

A new 109 year numerical wind-wave hindcast is developed for the North Atlantic Ocean based on the 20th century atmospheric reanalysis (20CR). Wave results are validated directly against data originating from voluntary observing ships and satellite altimetry in the North-East Atlantic Ocean. The normalized error for yearly-mean significant wave height (H_s) is shown to be of the order of 5% for the second part of the 20th century. An indirect validation is also performed through 10 m wind speed and suggests that the accuracy of yearly-mean H_s only slightly decreases for the beginning of the 20th century. The comparison between H_s and the index of the North Atlantic Oscillation revealed that this phenomenon partly controls H_s inter-annual variability, with a positive (negative) correlation in the northeastern (southwestern) part of the study area. The analysis of model results shows an increase in H_s over the whole North Atlantic Ocean superimposed to the inter-annual variability, reaching 0.01 m.yr^{-1} (20 to 40% over the 20th century) north of 50°N . This increase is explained by a rise in wind speed exceeding 20% north of 50°N . The roughening in the wave climate demonstrated in this study is expected to have strong implications for the development of coastal zones and could explain the increase in erosion along the North Atlantic shorelines.

© 2013 Elsevier B.V. All rights reserved.

1. Introduction

Ocean wind-waves are relevant for numerous engineering and scientific questions, both in coastal zones and in the deep ocean. Nevertheless, the proper characterization of wave height inter-annual variability and the depiction of long-term trends require long-term times series while wave data are almost inexistent prior to 1950. Compared to local measurements, wave height data derived from satellite (Bauer et al., 2001; Woolf et al., 2002) offers the unique advantage of a global coverage. Thus, Young et al. (2011) found a general global upward trend for wind speed and significant wave height (H_s) over the period 1985–2008, this rate being larger for the 90th and 99th percentiles. However, the 24-year covered period is too short to conclude whether this upward trend results from inter-annual or inter-decadal variability or a long term trend driven by global change. Wave height derived from Voluntary Observing Ships (hereafter VOS) was shown to constitute an interesting approach (Gulev et al., 2003; Gulev and Grigorjeva, 2004), although observations are restricted mostly to the main commercial routes and become very scarce prior to 1950. Alternatively, the availability of long-term atmospheric reanalyses, such as the ERA-40 project (Uppala et al., 2005) or the NCEP/NCAR project (Kalnay et al., 1996) together with significant improvements of the

predictive skills of wind-wave models (e.g. Janssen, 2008) allowed for the development of accurate long-term numerical hindcasts (Cox and Swail, 2001; Dodet et al., 2010; Reistad et al., 2011; Charles et al., 2012; Reguero et al., 2012). Dodet et al. (2010) showed an increase in wave height reaching up to 0.02 m.yr^{-1} in the North-East Atlantic Ocean over the period 1952–2010, although this increase was partly associated with an increase in the North Atlantic Oscillation (hereafter NAO) index (Hurrell, 1995) over this period. The recent availability of the twentieth century atmospheric reanalysis (hereafter 20CR, Compo et al., 2011) provides the unique opportunity to extend a wave hindcast over the whole 20th century. This study presents the results of a new numerical wave hindcast spanning from 1900 to 2008 and investigates the existence of long term trends superimposed on the inter-annual variability.

2. Methods and data

2.1. The numerical model

We developed a new numerical wave hindcast based on the spectral wave model WaveWatch III (Tolman, 2009), which solves the wave action equation on regular grids using finite differences. A 1° resolution computational grid was implemented over the North Atlantic Ocean (80°W – 10°E ; 0°N – 80°N , Fig. 1). The physical and numerical parameterizations are the same as described by Dodet et al. (2010). Sea-ice modifies the fetch according to a seasonal cycle and was thus taken into account. Sea-ice data provided with the 20CR reanalysis was only available at a 1.875° spatial resolution, which is

^{*} Corresponding author. Tel.: +33 546507636; fax: +33 546458274.
E-mail address: xbertin@univ-lr.fr (X. Bertin).

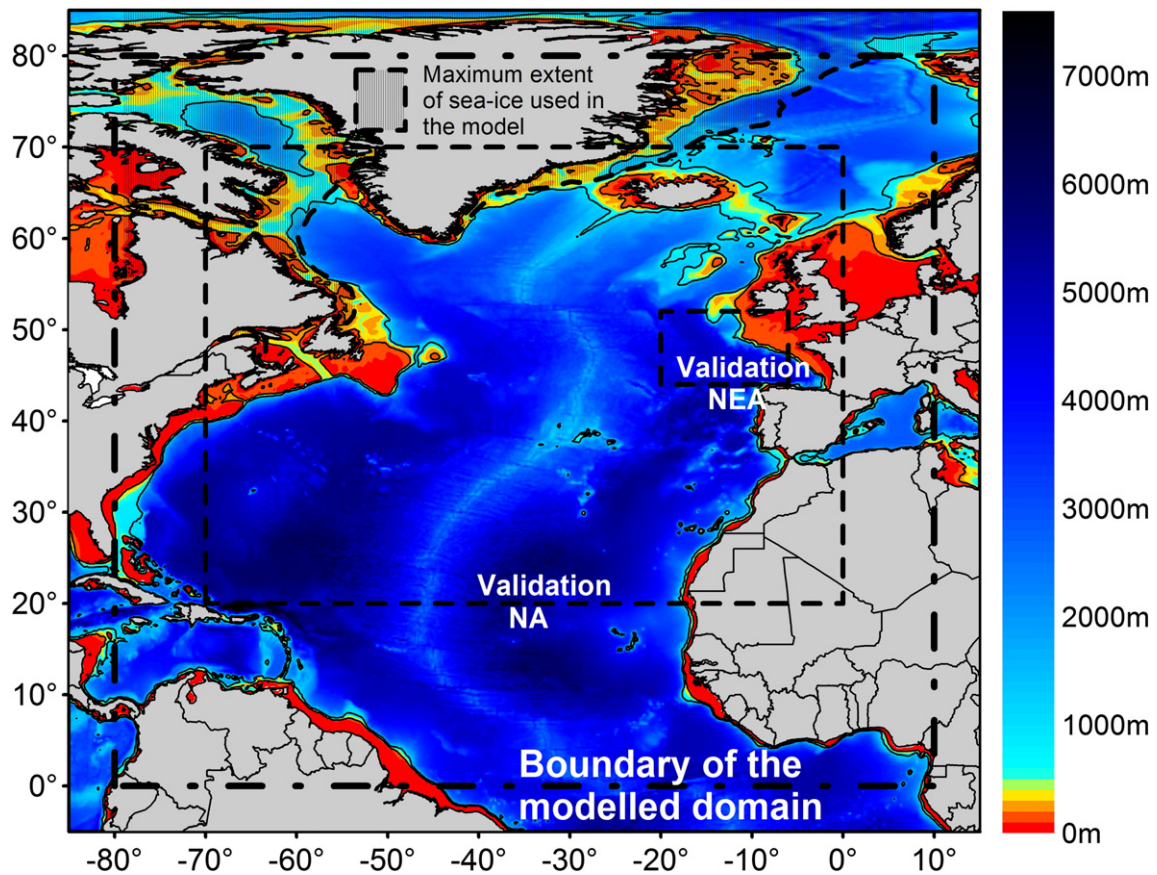


Fig. 1. Bathymetric map of the North Atlantic Ocean. The dash-dotted rectangle corresponds to the extent of the computational grid, the dashed rectangle corresponds to the validation of NA and NEA to the areas over which VOS data were integrated and the dashed area corresponds to the maximum extent of sea-ice as used in the model.

too coarse for our numerical hindcast. Alternatively, we defined an annual synthetic cycle with a 1-month interval averaging high-resolution (0.5°) sea-ice predictions over the period 1982–2010 (Fig. 1) originating from the NOAA OI SST V2 reanalysis (Reynolds et al., 2007). The model was forced with 3-hourly wind fields originating from the 20CR reanalysis V2 (Compo et al., 2011). This atmospheric reanalysis assimilates pressure observation and the data considered in this study corresponds to the ensemble-mean data provided over a $1.875^\circ \times 1.875^\circ$ grid. However, 20CR ensemble-mean wind fields are expected to be too smooth in the end of the 19th century (Wang et al., in press), which is a major limitation to force a dynamical wave hindcast. In particular, extreme winds from the ensemble-mean were shown to be low-biased (Bronnimann et al., 2012) for this period. These limitations explain why this study was restricted to the analysis of yearly-mean wave heights in the 20th century.

Finally, 3-hourly time series of wave heights were archived at each grid node and long-term trends were computed using a Huber robust regression method (Huber, 1981). This analysis was restricted to an area spanning 70°W – 10°E and 20°N – 70°N (Fig. 1), which corresponds to the area where field observations were available for validation.

2.2. Validation of input wind fields

The key issue when performing a wave hindcast over such a long period is the consistency of the input wind fields along the time. In order to verify the quality of the 20CR reanalysis along the 20th century, we performed a point-by-point comparison with sea-level pressure (SLP) and 10 m wind speed (U_{10}) originating from VOS data reported in the ICOADS database (International Comprehensive

Ocean–Atmosphere Data Set, Woodruff et al., 2011). This data was not assimilated in the 20CR and thereby allows for an independent validation. An inter-comparison between SLP and U_{10} originating from the popular ERA40 ($2.5^\circ \times 2.5^\circ/6$ h) and the NCEP/NCAR ($1.875^\circ \times 1.875^\circ/6$ h) reanalyses was also performed over the period of ERA40 (1958–2001). For each year, the root mean square of the difference (hereafter RMSD) between modeled (20CR, NCEP/NCAR and ERA40) and observed (VOS) SLP and U_{10} was performed over the North Atlantic Ocean (70°W – 0°W and 20°N – 70°N , Fig. 1). This area includes a large density of observations, ranging from a few tens per year in the late 19th century to several hundreds of thousands for the last 6 decades.

This comparison reveals firstly a good agreement between observed and modeled SLP for the three considered atmospheric reanalyses, with a root mean square of the difference (hereafter RMSD) of the order of 2 hPa from 1950 to 1990, decreasing to less than 1.5 hPa for the last decade (Table 1; Fig. 2A). This RMSD increases by 15% for the 20CR reanalysis for the first half of the 20th century, although two orders of magnitude less observations were available over the period 1900–1920. The comparison between observed and modeled U_{10} for the three selected reanalyses shows that RMSD is of the order of 3.5 m/s for the period 1950–2010, with a slight decrease over the last decade (Table 1; Fig. 2B). In more details, ERA40 performs slightly better than 20CR and NCEP, although the comparison shows a larger negative bias of the order of 2.0 m/s (Table 1). Low-biased winds in ERA40 were already reported by Reistad et al. (2011). RMSD and NRMSD for U_{10} originating from 20CR only show a 10% increase for the period 1900–1950 compared to the second part of the 20th century. Finally, the comparison between 20CR reanalysis and VOS data for the end of the 19th century reveals that both SLP and U_{10} have much larger errors

Table 1

Statistical errors of model/data comparison for yearly-mean sea-level pressure (SLP), wind speed (U_{10}) and wave height: root mean square error (RMSE), normalized root mean square error (NRMSE) and bias (m). For NCEP and 20CR, H_s referred to modeled wave height using wind fields originating from these databases.

Period	Database	SLP			U_{10}			Yearly-mean H_s		
		RMSD (hPa)	NRMSE (%)	BIAS (hPa)	RMSD ($m.s^{-1}$)	NRMSE (%)	BIAS ($m.s^{-1}$)	RMSD (m)	NRMSE (%)	BIAS (m)
1958–2001	NCEP	1.9	0.19	−0.06	3.71	37	−1.29	0.13	3.9	0.00
	ERA40	1.82	0.18	−0.06	3.42	35	−2.02	0.51	16.2	−0.50
	20CR	2.21	0.25	0.22	3.58	36	−0.94	0.18	5.8	0.11
1900–1950	20CR	2.43	0.23	0.11	3.91	39	−0.79	/	/	/

for this period, although too few observations are available to quantify them properly. This large uncertainty supports the limitation of our analysis to the 20th century.

2.3. Validation of wave predictions

In order to validate wave model predictions, we used wave height data derived from VOS and processed by Gulev and Grigorieva (2004). Data after 1950 provides separate estimates of wind sea and swell. The corresponding significant wave height (H_s) was computed as the square root of the sum of the square of wind sea and swell heights. This resulting wave height is thus consistent with the spectral H_s computed with the model. Unlike the point-by-point comparison for SLP and U_{10} , H_s was integrated in space and time, which reduces the random part of the uncertainty associated with wave height visual estimation (e.g. Gulev et al., 2003). Yearly-mean modeled H_s was then integrated over a box spanning 20°W–6°W and 44°N–52°N. This area was selected because it corresponds to the area where the largest number of observation is available in the North Atlantic Ocean. Statistical errors were computed between model results and observations (Fig. 3, Table 1). Years with less than one observation everyday were arbitrarily removed from the computation. Model results were also compared against the wave hindcast of Dodet et al. (2010) that uses NCEP/NCAR wind fields, and wave height originating from the ERA40 reanalysis. Direct model validation prior to 1950 was not possible because VOS

reports are scarce before this date and officers only reported the highest wave component, which is not consistent with our modeled H_s .

The comparison between observed and modeled yearly-mean H_s over the period 1956–2010 shows a good agreement with a root mean square of the difference (RMSD) of 0.19 m (5.6% once normalized by the observations, hereafter NRMSE) and a small bias of 0.11 m (Fig. 3, Table 1). The hindcast of Dodet et al. (2010) slightly better matches the observations with an RMSD of 0.12 m (3.6% NRMSE) and a nil bias. H_s from ERA40 has a much larger error, mainly due to a 0.5 m negative bias, which may be related to the 2.0 m/s negative bias in U_{10} shown above. Since the use of VOS data to validate our wave hindcast is unpublished to date and could thus be questionable, we also performed a comparison with yearly-mean wave heights computed from satellite altimetry and retrieved from the GlobWave database (www.globwave.org). This comparison (Fig. 3) reveals a good agreement with VOS and numerical hindcast, with only a 0.10 to 0.15 m negative bias. The inter-annual variability of wave height is fairly consistent from one method to another (numerical hindcast, VOS and altimetry), with Pearson correlation coefficients ranging from 0.73 to 0.82.

3. Results

Mean H_s over the period 1900–2008 is shown on the upper panel of Fig. 4A. This figure reveals that, in the North Atlantic Ocean, the

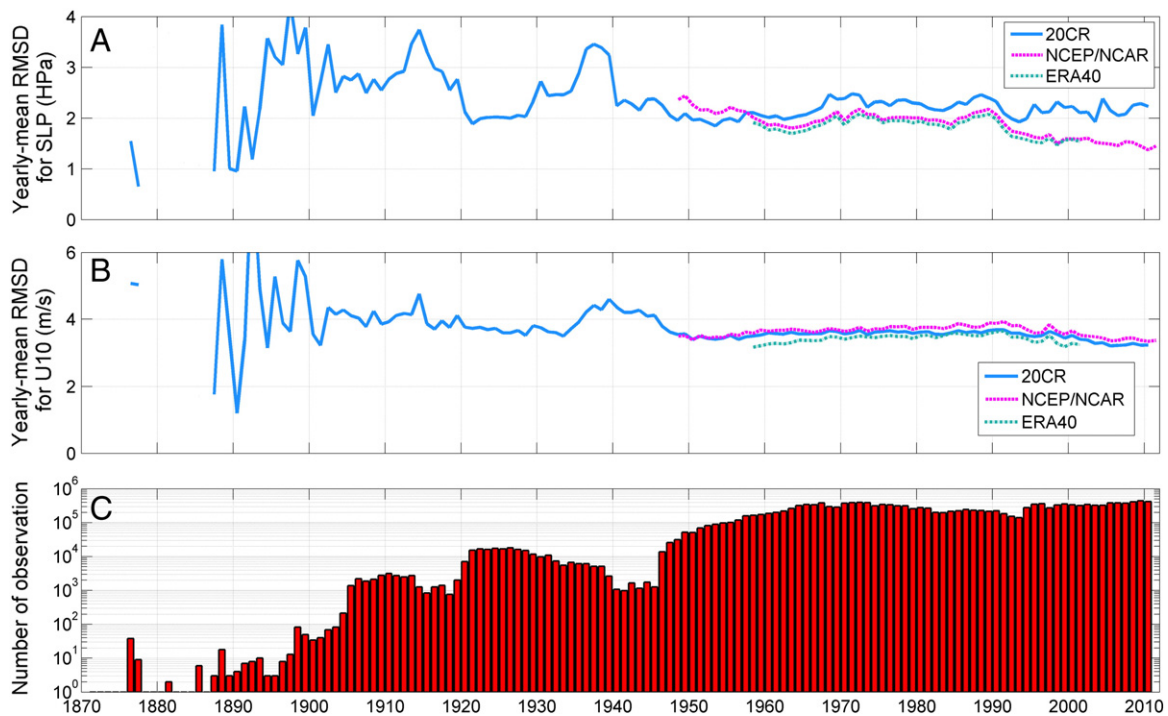


Fig. 2. Yearly time series of root mean square difference between observed (VOS data) and modeled (20CR, NCEP/NCAR and ERA40 reanalyses) SLP (A), U_{10} (B) and number of observations per year used for this comparison performed in the North Atlantic Ocean (0°W–70°W; 20°N–70°N) (C).

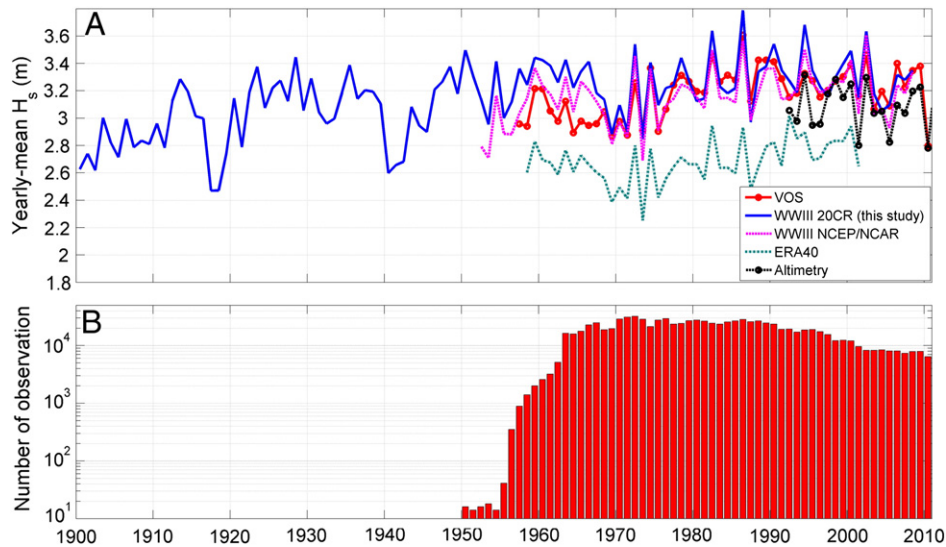


Fig. 3. Comparison between observed and modeled yearly-mean H_s (A) and (B) number of observations per year in the NEA used for this comparison.

largest mean H_s is found at northern latitudes (40° to 60°N), with maximum values over 3.5 m. To the South, mean H_s decreases progressively to about 2.0 m. Linear trends for H_s were computed over the period 1900–2008 and the results are shown on Fig. 4B. A clear global increase can be seen all over the North Atlantic Ocean and the trends are significant almost everywhere at more than 95% (F-test) to the North of 30°N . In more details, the trends are larger at Northern latitudes (between 50°N and 70°N) with values exceeding locally 0.01 m.yr^{-1} . Such trends are equivalent to an increase of more than 1.0 m over the studied period, which corresponds locally to a more than 40% increase of the yearly-mean value. These upward trends decrease to the South to less than 0.005 m.yr^{-1} but combined with lower yearly-mean H_s , these trends still represent a 15% increase over the period 1900–2008.

In order to tentatively explain these trends, Pearson correlation coefficients were computed between the yearly-mean station-based NAO index (Hurrell, 1995) and yearly-mean H_s (Fig. 4C). These correlation maps reveal a significant (at more than 95%) and large positive correlation area to the North-East of the study area, with correlation coefficients exceeding 0.5. A significant negative correlation area develops between 30° and 40°N , with correlation coefficients reaching -0.5 . Finally, a last significant and weakly positive correlation area developed to the South-East of the study area, with correlation coefficients reaching 0.3.

To distinguish between linear trends and inter-annual variability driven by the NAO, a decomposition in Empirical Orthogonal Functions (hereafter EOFs; Preisendorfer, 1988) of yearly-mean time series of H_s was performed (Fig. 5). This analysis shows that the 1st mode of decomposition explains 74% of the total variance of yearly-mean H_s . The corresponding spatial pattern of this mode (Fig. 5A) matches closely that of the linear trends of Fig. 4B. The time-series of the first EOF confirms that this mode corresponds to the increase in H_s over the studied period. In details, the increase is strong during a first period from 1900 to 1960, followed by a second period from 1960 to 2008 where the increase is much weaker. The second mode of decomposition (Fig. 5B) explains 9% of the total variance of yearly-mean H_s and the associated spatial pattern strongly matches that of the correlation map between yearly-mean H_s and NAO index (Fig. 4C). This agreement is confirmed by the associated time-series, which is well correlated with the yearly-mean NAO index ($R^2 = 0.73$, Fig. 5B) although the correlation drops between 1920 and 1930. In order to better quantify this behavior, Pearson correlation coefficients were computed over a 10 year sliding window, which reveals that correlation coefficients range from 0.6 to 0.9 over the whole period and drop to 0.45 from 1920 to 1930.

4. Discussion and conclusions

4.1. Significance of the trends

This study relies on a new numerical wave hindcast, driven by wind fields originating from the 20CR reanalysis starting in 1900. A validation of wave predictions after 1955 was undertaken based on VOS and revealed that errors for yearly-mean H_s were of the order of 5%. A similar direct validation prior to 1950 was not possible since, according to the author's knowledge, wave measurements or consistent observation is insufficiently available. This difficulty questions the reliability of our results for the period 1900–1955, although the 20CR reanalysis was shown to be homogeneous for the North Atlantic over the 20th century (Wang et al., in press). Alternatively, U_{10} originating from the 20CR reanalysis was compared against measurements from VOS, which revealed that errors on this parameter only increased by 10% for the first half of the 20th century. Nevertheless, the values of RMSD for U_{10} (around 3.5 m.s^{-1}) are 50% larger compared to the values usually obtained when comparing atmospheric reanalysis with buoys (e.g. Chawla et al., in press) or satellite scatterometer (e.g. Dee et al., 2011; Durrant et al., in press). In addition to the probably weaker quality of VOS data compared to buoy modern measurements or scatterometers, this difference may originate from the interpolations in space (the three atmospheric reanalyses have spatial resolutions of the order of 2°) and in time (3- to 6-hourly data) associated with our RMSD computation. However, the comparison between VOS and 20CR aimed at investigating how much U_{10} used to drive our wave hindcast deteriorates over the studied period time rather than providing an absolute validation of the 20CR reanalysis.

It is accepted that the dependence of H_s on the wind speed U obeys a relationship of the form $H_s \approx U^\beta$, where β is a coefficient varying between 1 for short-fetch limited conditions and 2 for fully developed seas (Ardhuin et al., 2007; Janssen, 2008). In this study, the $\sim 10\%$ larger errors in wind speed for the first half of the 20th century would increase the NRMSE in H_s from 5% for the period 1950–2008 to 6% for the period 1900–1950. Consequently, the 20 to 40% increases in H_s that we demonstrated over the North Atlantic Ocean still hold robustly.

4.2. Comparison with previous studies

Several studies have already reported increases in H_s in the North Atlantic Ocean (Bacon and Carter, 1991; Wang and Swail, 2001; Doded et al., 2010; Le Cozannet et al., 2011) over the last decades. Nevertheless,

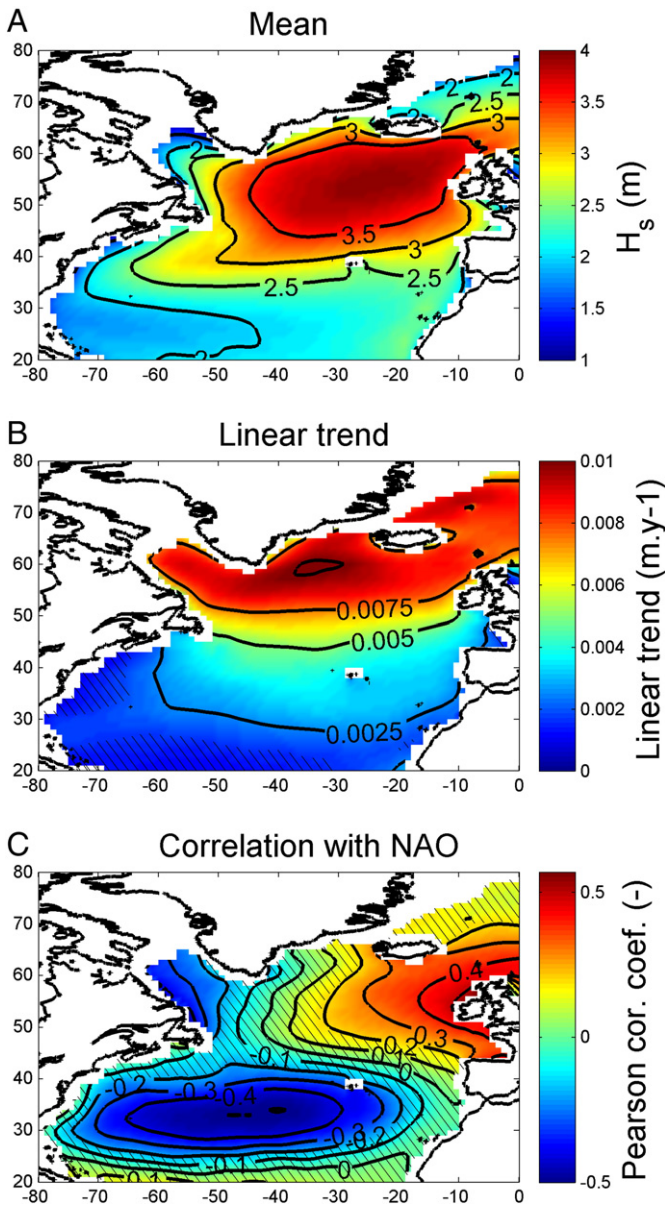


Fig. 4. (A) Mean H_s , (B) linear trend for H_s and (C) Pearson correlation coefficient between yearly-mean H_s and station based NAO index. The hatched areas correspond to areas where trends (F-Test) and correlations are not significant at least at a 95% confidence level.

the inter-annual variability of H_s at northern latitudes was shown to be partly controlled by the NAO and the reported upward trends in H_s were to some extent explained by a strong increase in the NAO index over the last 6 decades (Woolf et al., 2002; Dodet et al., 2010). In this study, a significant and positive correlation between H_s and the NAO index was also identified in the North-East Atlantic Ocean, although weaker than in Dodet et al. (2010) who used winter-mean parameters. Unlike previous studies focused on the last 5 to 6 decades, the NAO index does not experience any significant trend over the period 1900–2008. This implies that the large increase in H_s (up to more than 40%) demonstrated over the whole North Atlantic Ocean cannot be explained by the NAO. Our interpretation is that a long-term upward trend is superimposed on the partly NAO-controlled inter-annual variability of H_s . This hypothesis is corroborated by the EOF analysis, which shows that the dominant mode is clearly correlated with the spatial and temporal variations of the upward trend (Fig. 5A). The spatial patterns and the magnitude of our trends differ from those of Wang et al.

(2012), who statistically reconstructed H_s over the North Atlantic Ocean for the period 1871–2010 based on SLP originating from 20CR. Nevertheless, their study investigates a different period of time and different wave parameters (seasonal means and maximum), which turns delicate the comparison with our study.

On the other hand, the order of magnitude of the upward trends we found in the North Atlantic Ocean matches the findings of other studies in other region of the world's ocean. Thus, Reguero et al. (2013) performed a wave numerical hindcast around Latin America based on NCEP/NCAR U_{10} and found trends reaching locally 0.01 m.yr^{-1} for the period 1948–2012. In the North-East Pacific Ocean, Ruggiero et al. (2010) used wave buoy measurements and found a 0.015 m.yr^{-1} increase for the yearly-mean H_s over the last 35 years. This value is corroborated by the findings of Gulev and Grigorieva (2004) who found a 0.01 m.yr^{-1} increase in this region using VOS over the period 1900–2002.

4.3. Causes for H_s increase

Wind speed from the 20CR reanalysis showed an $8 \pm 2\%$ increase in the North-East Atlantic Ocean (validation NEA, Fig. 1) over the period 1900–2008 ($-0.07\%.\text{yr}^{-1}$). This upward trend is partly corroborated by VOS, which showed a $13 \pm 2\%$ increase over the period 1904–2010 ($-0.1\%.\text{yr}^{-1}$, Fig. 6). Over the shorter period 1948–2010, wind speed from NCEP/NCAR also shows a $7 \pm 1\%$ increase ($-0.1\%.\text{yr}^{-1}$).

Donat et al. (2011) investigated the occurrence of wind storm using the same atmospheric reanalysis and depicted an upward trend in storm activity for northern and western Europe over the period 1871–2008. Trends in wind speed were also computed over the whole North Atlantic Ocean and this analysis revealed a generalized increase in U_{10} , ranging from 5 to 15% (0.05 to $0.13\%.\text{yr}^{-1}$) at intermediate latitudes and reaching 20 to 40% (0.2 to $0.4\%.\text{yr}^{-1}$) over a band spanning from 50°N to 70°N . These upward trends in wind speed directly explain the upward trends in H_s described in the previous section. Unfortunately, based on this study, it was not possible to determine the causes for the upward trends in wind speed identified over the North Atlantic Ocean. On the one hand, several authors found that global warming would only induce minor changes in the frequency and intensity of mid-latitude storms (Ulbrich et al., 2008; Bengtsson et al., 2009). On the other hand, other studies relying on climate model experiments (e.g. Donat et al., 2010) have suggested that enhanced greenhouse gas forcing would yield more frequent and stronger wind storms. Under this absence of consensus, we cannot rule out the possibility that the increase in wind speed and wave height identified over the North Atlantic Ocean could result, at least partly, from the increase in greenhouse gas concentrations over the last centuries.

4.4. Consequences of these results

In addition to direct consequences on navigation, offshore engineering and even climate dynamics due to wave-induced heat and mass fluxes (e.g., through wave-induced turbulence, drag modification and aerosols), the increase in H_s in the North Atlantic Ocean that we demonstrated in this study has strong implications on coastal zone dynamics. Thus, the increase in coastal erosion observed in western Europe over the last century (e.g. EuroSION, 2003) could be related to the roughening of the wave climate at northern latitudes and not only to long-term sea-level rise (Bruun, 1962) and decrease in sediment supply from rivers due to dams. This hypothesis matches the recent conclusions of Ruggiero (2013), who proposed that the wave height increases in the NE Pacific have had a more significant role in the increased coastal erosion than sea level rise. To investigate this hypothesis further, one promising perspective would be to force coastal area morphodynamic models (e.g. Lesser et al., 2004; Bertin et al., 2009) with time series of wave spectra originating from the hindcast presented in this study. This data

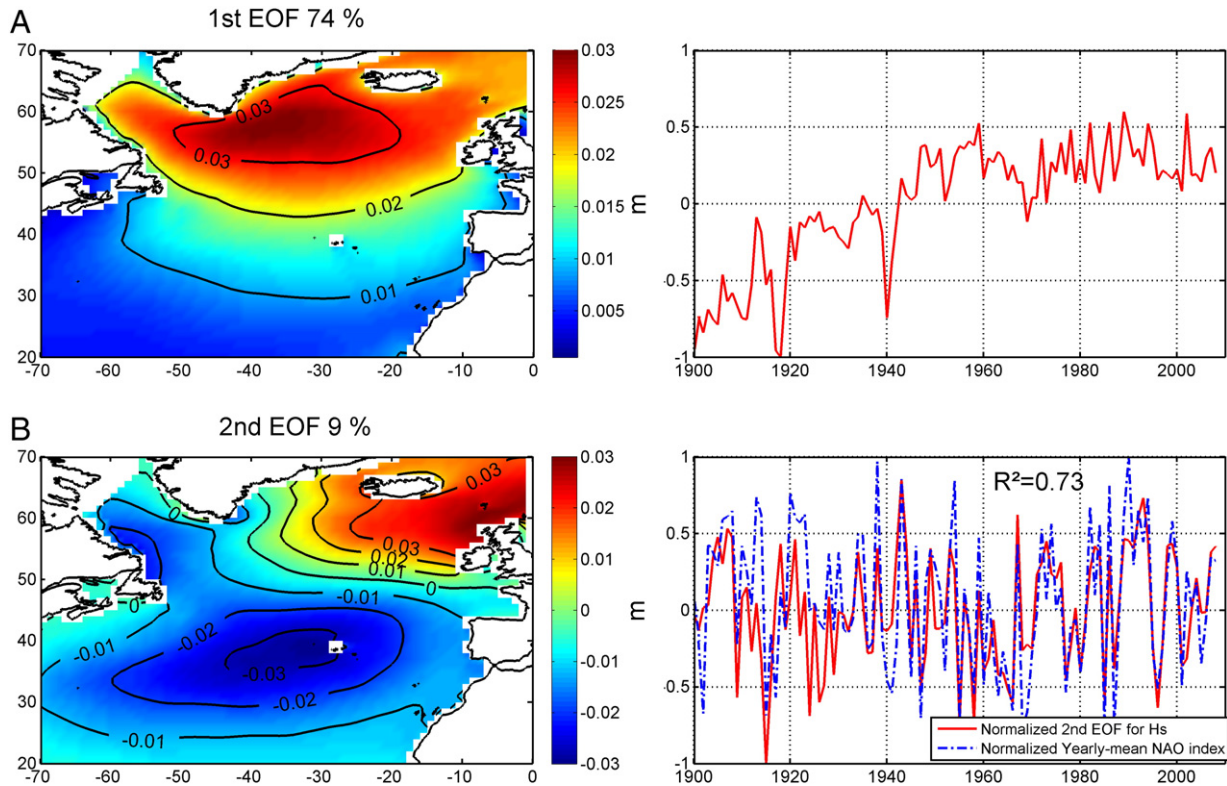


Fig. 5. (A) EOF 1st mode of decomposition of yearly-mean H_s (left) and time-series of normalized EOF1 (right). (B) EOF 2nd mode of decomposition of yearly-mean H_s (left) and time series (right) of normalized EOF2 and station based NAO index.

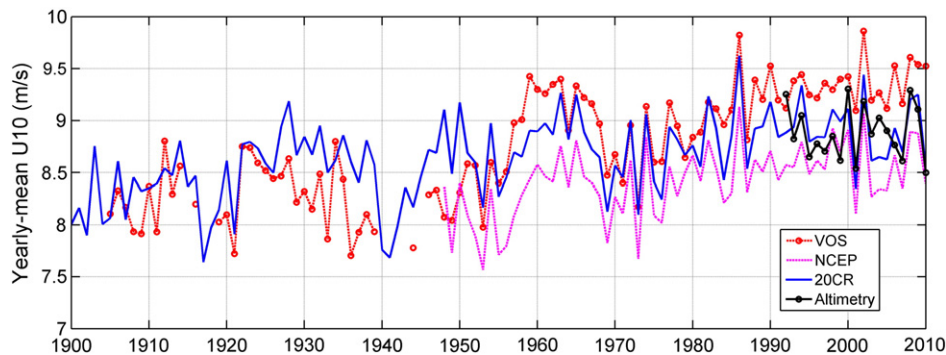


Fig. 6. Yearly-mean wind speed in the NEA (Fig. 1) from VOS data, 20CR and NCEP reanalyses and satellite altimetry.

will be available for the community in a near future through SONEL (www.sonel.org).

Acknowledgments

This study wouldn't have been possible without the availability of the 20th century reanalysis, supported by the US Department of Energy, Office of Science Innovative and Novel Computational Impact on Theory and Experiment (DOE INCITE) program, and Office of Biological and Environmental Research (BER), and by the National Oceanic and Atmospheric Administration Climate Program Office. IFREMER is acknowledged for making available quality-checked altimetry data through the GlobWave project. The authors thank the developing team of the model WaveWatch III. Finally, Vika Grigorjeva (Shirshov Institute of Oceanology, Moscow, Russia) is greatly acknowledged for providing us the VOS data. The investigation of past wave climates

was part of the project ANR JC DYNAMO (agreement n° ANR-12-JS02-00008-01).

References

- Arduin, F., Bertotti, L., Bidlot, J.-R., Cavaleri, L., Filipetto, V., Lefevre, J.-M., Wittmann, P., 2007. Comparison of wind and wave measurements and models in the Western Mediterranean Sea. *Ocean Engineering* 34 (3–4), 526–541.
- Bacon, S., Carter, D.J.T., 1991. Wave climate changes in the north Atlantic and North Sea. *International Journal of Climatology* 11, 545–558.
- Bauer, E., 2001. Interannual changes of the ocean wave variability in the North Atlantic and in the North Sea. *Climate Research* 18, 63–69.
- Bengtsson, L., Hodges, K.I., Keenlyside, N., 2009. Will extratropical storms intensify in a warmer climate? *Journal of Climate* 22, 2276–2301.
- Bertin, X., Fortunato, A.B., Oliveira, A., 2009. Simulating morphodynamics with unstructured grids: description and validation of an operational model for coastal applications. *Ocean Modelling* 28, 75–873.
- Bronnimann, S., Martius, O., Von Waldow, H., Welker, C., Luterbacher, J., Compo, G.P., Sardeshmukh, P.D., Usbeck, T., 2012. Extreme winds at northern mid-latitudes since 1871. *Meteorologische Zeitschrift* 21 (1), 13–27.

- Bruun, P., 1962. Sea level rise as a cause of shore erosion. *Journal of Waterways, Ports and Harbors Division* 88 (1–3), 117–130.
- Charles, E., Idier, D., Thiébot, J., Le Cozannet, G., Pedreros, R., Ardhuin, F., Planton, S., 2012. Present wave climate in the Bay of Biscay: spatiotemporal variability and trends from 1958 to 2001. *Journal of Climate* 25 (6), 2020–2039.
- Chawla, A., Spindler, D.M., Tolman, H.L., 2013. Validation of a thirty year wave hindcast using the Climate Forecast System Reanalysis winds. *Ocean Modelling* (in press).
- Compo, G.P., Whitaker, J.S., Sardeshmukh, P.D., Matsui, N., Allan, R.J., et al., 2011. The twentieth century reanalysis project. *Quarterly Journal of the Royal Meteorological Society* 137, 1–28.
- Cox, A.T., Swail, V.R., 2001. A global wave hindcast over the period 1958–1997: validation and climate assessment. *Journal of Geophysical Research C: Oceans* 106 (C2), 2313–2329.
- Dee, D.P., et al., 2011. The ERA-interim reanalysis: configuration and performance of the data assimilation system. *Quarterly Journal of the Royal Meteorological Society* 137 (656), 553–597.
- Dodet, G., Bertin, X., Taborda, R., 2010. Wave climate variability in the North-East Atlantic Ocean over the last six decades. *Ocean Modelling* 31, 120–131.
- Donat, M.G., Leckebusch, G.C., Pinto, J.G., Ulbrich, U., 2010. European storminess and associated circulation weather types: future changes deduced from a multi-model ensemble of GCM simulations. *Climate Research* 42, 27–43. <http://dx.doi.org/10.3354/cr00853>.
- Donat, M.G., Renggli, D., Wild, S., Alexander, L.V., Leckebusch, G.C., Ulbrich, U., 2011. Reanalysis suggests long-term upward trends in European storminess since 1871. *Geophysical Research Letters* 38. <http://dx.doi.org/10.1029/2011GL047995> (L14703).
- Durrant, T.H., Greenslade, D.J.M., Simmonds, I., 2013. The effect of statistical wind corrections on global wave forecasts. *Ocean Modelling* (in press).
- EuroSION, 2003. Trends of coastal erosion in Europe. EuroSION Project, Final Version Report. (Available at: <http://www.euroSION.org>).
- Gulev, S., Grigorieva, V., 2004. Last century changes in ocean wind wave height from global visual wave data. *Geophysical Research Letters* 31. <http://dx.doi.org/10.1029/2004GL021040> (L24302).
- Gulev, S., Grigorieva, V., Sterl, A., Woolf, D., 2003. Assessment of the reliability of wave observations from voluntary observing ships: insights from the validation of a global wind wave climatology based on voluntary observing ship data. *Journal of Geophysical Research* 108, 3236. <http://dx.doi.org/10.1029/2002JC001437>.
- Huber, P.J., 1981. *Robust Statistics*. John Wiley & Sons, Inc., Hoboken, NJ.
- Hurrell, J.W., 1995. Decadal trends in the North Atlantic Oscillation: regional temperatures and precipitations. *Science* 269, 676–679.
- Janssen, P.A.E.M., 2008. Progress in ocean wave forecasting. *Journal of Computational Physics* 227 (7), 3572–3594.
- Kalnay, E., Kanamitsu, M., Cistler, R., Collins, W., Deaven, D., Gandin, L., Iredell, M., Saha, S., White, G., Woolen, J., Zhu, Y., Chelliah, M., Ebisuzaki, W., Higgins, W., Janowiak, J., Mo, K., Ropelewski, C., Wang, J., Leetma, A., Reynolds, R., Jenne, R., Joseph, D., 1996. The NCEP/NCAR reanalysis project. *Bulletin of the American Meteorological Society* 77, 437–471.
- Le Cozannet, G., Lecacheux, S., Delvallee, E., Desramaut, N., Oliveros, C., Pedreros, R., 2011. Teleconnection pattern influence on sea-wave climate in the Bay of Biscay. *Journal of Climate* 24 (3), 641–652.
- Lesser, G.R., Roelvink, J.A., Van Kester, J.A.T.M., Stelling, G.S., 2004. Development and validation of a three-dimensional morphological model. *Coastal Engineering* 51, 883–915.
- Preisendorfer, R.W., 1988. *Principal Component Analysis in Meteorology and Oceanography*. Elsevier, Amsterdam (436 pp.).
- Reguero, B.G., Menéndez, M., Méndez, F.J., Mínguez, R., Losada, I.J., 2012. A global ocean wave (GOW) calibrated reanalysis from 1948 onwards. *Coastal Engineering* 65, 38–55.
- Reguero, B.G., Méndez, F.J., Losada, I.J., 2013. Variability of multivariate wave climate in Latin America and the Caribbean. *Global and Planetary Change* 100, 70–84.
- Reistad, M., Breivik, Ø., Haakenstad, H., Aarnes, O.J., Furevik, B.R., Bidlot, J., 2011. A high-resolution hindcast of wind and waves for the North Sea, the Norwegian Sea, and the Barents Sea. *Journal of Geophysical Research* 116. <http://dx.doi.org/10.1029/2010JC006402> (C05019).
- Reynolds, R.W., Smith, T.M., Liu, C., Chelton, D.B., Casey, K.S., Schlax, M.G., 2007. Daily high-resolution-blended analyses for sea surface temperature. *Journal of Climate* 20, 5473–5496.
- Ruggiero, P., 2013. Is the intensifying wave climate of the U.S. Pacific Northwest increasing flooding and erosion risk faster than sea-level rise? *Journal of Waterway, Port, Coastal, and Ocean Engineering* 139 (2), 88–97.
- Ruggiero, P., Komar, P.D., Allan, J.C., 2010. Increasing wave heights and extreme value projections: the wave climate of the U.S. Pacific Northwest. *Coastal Engineering* 57, 539–552.
- Tolman, H.L., 2009. User manual and system documentation of WAVEWATCH III version 3.14. NOAA/NWS/NCEP/MMAB Technical Note 276. (194 pp.).
- Ulbrich, U., Pinto, J.G., Kupfer, H., Leckebusch, G.C., Spanghel, T., Reyers, M., 2008. Changing Northern Hemisphere storm tracks in an ensemble of IPCC climate change simulations. *Journal of Climate* 21, 1669–1679.
- Uppala, S., Kallberg, P., Simmons, A., da Costa, Andrae U., Bechtold, V., Fiorino, M., Gibson, J., Haseler, J., Hernández, A., Kelly, G., 2005. The era-40 reanalysis. *Quarterly Journal of the Royal Meteorological Society* 131, 2961–3012.
- Wang, X., Swail, V., 2001. Trends of Atlantic wave extremes as simulated in a 40-yr wave hindcast using kinematically reanalyzed wind fields. *Journal of Climate* 15, 1020–1035.
- Wang, X.L., Feng, Y., Swail, V.R., 2012. North Atlantic wave height trends as reconstructed from the 20th century reanalysis. *Geophysical Research Letters* 39 (18) (L18705).
- Wang, X.L., Feng, Y., Compo, G.P., Swail, V.R., Zwiers, F.W., Allan, R.J., Sardeshmukh, P.D., 2013. Trends and low frequency variability of extra-tropical cyclone activity in the ensemble of twentieth century reanalysis. *Climate Dynamics*. <http://dx.doi.org/10.1007/s00382-012-1450-9> (in press).
- Woodruff, S.D., Worley, S.J., Sandra, J., Lubker, S.J., Ji, Z., Freeman, J.E., Berry, D.I., Brohan, P., Kent, E.C., Reynolds, R.W., SR, Wilkinson C., 2011. ICOADS Release 2.5: extensions and enhancements to the surface marine meteorological archive. *International Journal of Climatology* 31, 951–967. <http://dx.doi.org/10.1002/joc.2103>.
- Woolf, D.K., Cotton, P.D., Challenor, P.G., 2002. Variability and predictability of the North Atlantic wave climate. *Journal of Geophysical Research* 107 (C10), 9–23.
- Young, I.R., Zieger, S., Babanin, A.V., 2011. Global trends in wind speed and wave height. *Science* 332 (6028), 451–455.